Coulomb interaction in quasibound states of graphene quantum dots

Zhong-Qiu Fu,[1] Ke-Ke Bai,[1,2] Ya-Ning Ren,[1] Jiao-Jiao Zhou,[3] and Lin He[1,*]

[1]*Center for Advanced Quantum Studies, Department of Physics, Beijing Normal University, Beijing 100875, People's Republic of China*

[2]*Institute of Physics, Hebei Normal University, Shijiazhuang 050024, People's Republic of China*

[3]*Department of Mathematics and Physics, Anhui Jianzhu University, Hefei 230601, People's Republic of China*

(Received 27 January 2020; revised manuscript received 29 April 2020; accepted 27 May 2020; published 11 June 2020)

Coulomb interaction is of central importance in localized energy levels (bound states) or electronic flat bands and can result in many exotic quantum phases. In a graphene monolayer, the relativistic massless Dirac fermion nature of the charge carriers enables us to realize unprecedented quasibound states, which are trapped temporarily via whispering-gallery modes (WGMs), in circular graphene quantum dots (GQDs). Here we show that Coulomb interaction still plays a dominating role in determining the electronic properties of the temporarily confined quasibound states with the lifetime (trapping time) of ∼10 fs. Our scanning tunneling microscopy and spectroscopy measurements demonstrate that the discrete quasibound state in a GQD will split into two peaks when it is partially filled. The energy separation of the two split peaks increases linearly with inverse effective radius of the GQDs, indicating that the splitting arises from the Coulomb interaction. Moreover, we show that the real-space distribution of the two split states separates in different regions of the GQD to reduce the Coulomb interaction, leading to the breaking of the WGM of the quasibound states.

DOI: 10.1103/PhysRevB.101.235310

I. INTRODUCTION

When the kinetic energy of the charge carriers is completely quenched or strongly suppressed, the Coulomb interaction can be dominant in determining electronic properties of the system, resulting in many exotic emergent quantum phases [1–15]. In quantum dots, it is well known that many interesting phenomena can be generated by the Coulomb interaction [12–20]. For example, Wigner crystal in graphene quantum dots (GQDs) was predicted to realization [19,20]. However, owing to the massless Dirac fermions' nature, the charge carriers in the graphene monolayer can only be temporarily confined to form quasibound states [21–29]. In circular GQDs, the massless Dirac fermions are temporarily confined into quasibound states via whispering-gallery modes (WGMs) because of the Klein tunneling in graphene [21–26]. The quasibound states differ from both the bound states and the flat bands because they have quite a short lifetime (trapping time), ∼10 fs [22,27]. Then, a fundamental question arises: Is the Coulomb interaction still important in determining the electronic properties of the quasibound states? In this work, we show that the Coulomb interaction is very important in the quasibound states. Our experiment demonstrates explicitly that the Coulomb interaction not only splits the partially filled quasibound states, but also breaks the WGMs of the corresponding quasibound states.

II. EXPERIMENT

In our experiment, a method is developed to obtain GQDs with different sizes in a continuous graphene sheet. The monolayer graphene was grown on a sulfur-rich copper foil by low-pressure chemical vapor deposition (LPCVD) [30]. During the high-temperature growth process, sulfur atoms segregate from the copper foils and form self-organized sulfur islands at the interface between graphene and copper foil (see Method and Fig. S1 of the Supplemental Material [31] for details of the sample preparation). According to our scanning tunneling microscopy (STM) experiments, the S atoms segregated from the Cu foil could form three typical structures on the metal surface, as summarized in Fig. 1, depending on the growth temperatures of the graphene. When we synthesized graphene at relative low temperature (1253–1273 K), the sulfur atoms tended to distribute randomly on the Cu surface as individual atoms, as shown in Figs. 1(a) and 1(d). With increasing the growth temperature to 1283–1303 K, the sulfur atoms formed well-ordered identical nanocluster superlattices, as shown in Figs. 1(b) and 1(e). By further increasing the growth temperature to 1313–1333 K, the sulfur atoms tended to assemble into nanoscale S islands, as shown in Figs. 1(c) and 1(f). Here we should point out that the growth of the graphene monolayer is not necessary for the formation of nanoscale S islands. In our experiment, we can obtain single-layer nanoscale S islands on a copper substrate by annealing the sulfur-rich copper foil at high temperature (see Fig. S2 [31]). The atomic-layer difference of graphene-Cu separations between inside and outside of the nanoscale S islands introduces sharp electronic junctions and, consequently, generates nanoscale GQDs in the continuous graphene monolayer.

III. RESULTS AND DISCUSSION

Figure 2(a) shows a representative STM topographic image of an individual GQD in a continuous graphene monolayer.

*helin@bnu.edu.cn

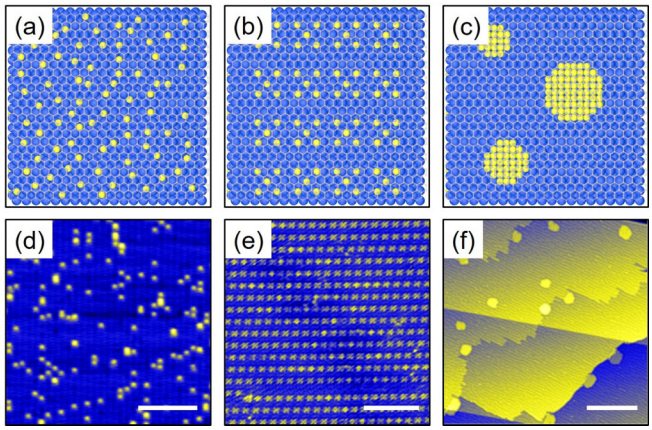

FIG. 1. Three typical structures formed by self-organized sulfur adatoms at the interface. (a), (d) Schematics and STM image of individual sulfur atoms distributed randomly at the interface between graphene and the copper substrate. (b), (e) Periodic sulfur nanoclusters formed at the interface. (c), (f) High-density sulfur islands formed at the interface between graphene and the copper substrate. Scale bars: 10 nm in (d), (e), 50 nm in (f).

The protuberance is generated by a sulfur island in the interface between the graphene and the copper substrate. The inset of Fig. 2(a) shows the height profile across the GQD and the height of the S atomic layer is measured as about 200 pm, which is consistent with that reported previously [32–34].

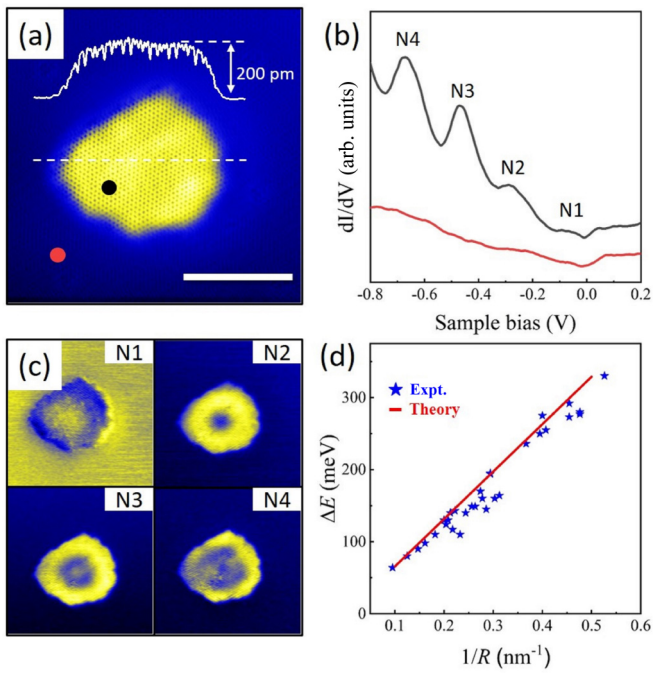

FIG. 2. Quasibound states in a GQD. (a) A STM topographic image of a GQD. Inset: Line profile along the white dashed line. (b) dI/dV spectra measured outside and inside of the GQD marked in panel (a). (c) STS maps recorded at the first four peaks in the dI/dV spectra of the GQD. (d) Plot of average level spacing for several resonant peaks as a function of the inverse effective radius for the GQDs. The red line is the theoretical result. Scale bar: 5 nm in (a).

Atomic-resolved STM measurement (Fig. S3 [31]) demonstrates the perfect continuity of the topmost graphene lattice with no signal of defect and no intervalley scattering around the GQD. Our field-emission resonance (FER) measurements, i.e., dz/dV spectra, indicate that the intercalation of sulfur islands introduces sharp electronic junctions between the inside and the outside of the nanoscale S island in the continuous graphene monolayer (see Fig. S4 for the details [31]). According to the energy shift of the first dz/dV peak (see Fig. S5 for the details [31]), the change of the local work function of graphene between the inside and the outside of the nanoscale S island is about 320 mV. Usually, the graphene on the copper surface is n doped (the Dirac point is about −300 mV) [22,24]. Besides, according to the potential difference on and off the island, we can determine that the graphene on the island is p doped and there is a p-n junction along the edge of the island.

Because of the Klein tunneling at the p-n junction, massless Dirac fermions in graphene will be reflected from the junction with high probability at large incident angles and these reflected quasiparticles will be confined temporarily into equally spaced quasibound states in the GQDs, which can be described by the WGM confinement [21–26]. In our experiment, a series of equally spaced quasibound states at negative energies are observed in the tunneling spectrum recorded in the GQD as shown in Fig. 2(b). Spatial-resolution scanning tunneling spectroscopy (STS) maps, which reflect the local density of states (LDOS) in real-space, show the spatial distribution of the quasibound states [Fig. 2(c)]. The lowest quasibound state exhibits a maximum near the center of the GQD, and higher quasibound states display shell structures and are progressively closer to the edge of the GQD as energy increases, directly demonstrating the confinement via the WGMs [22–24]. Our theoretical calculations, with considering the potential height about 320 meV and the radius of the GQD about 3.3 nm, as determined in the experiment, capture well the main features of the experimental results (see Fig. S6 and the Supplemental Material for the calculated method [31]), further confirming the WGM confinement of the massless Dirac fermions in the GQD. In our experiment, the WGM confinement of the massless Dirac fermions has been observed in all the studied GQDs. In the graphene monolayer, the confinement of the massless Dirac Fermions is analogous to Dirac particle in a circle and the average energy spacing of the quasibound states can be estimated as $\Delta E = \alpha \hbar v_F / R$, where α is a dimensionless constant of order unity, $\hbar$ is the reduced Planck's constant, $v_F = 1.0 \times 10^6$ m/s is the Fermi velocity of the graphene monolayer, and R is the effective radius of the GQDs. In Fig. 2(d), we summarize the energy spacing of the quasibound states ΔE as a function of the inverse effective radius $(1/R)$ of the GQDs, which agrees well with the confinement of the massless Dirac fermions in the GQDs [red line in Fig. 2(d)].

Usually, the Coulomb interaction manifests itself mainly around the Fermi level when the bound states or the flat bands are partially filled [1–20,35,36]. Previous studies demonstrated that the Coulomb interaction will split the partially filled bound state or flat band to lift the degeneracy of the studied system [1–20]. In our experiment, we find that the quasibound state splits into two peaks in the tunneling spectra

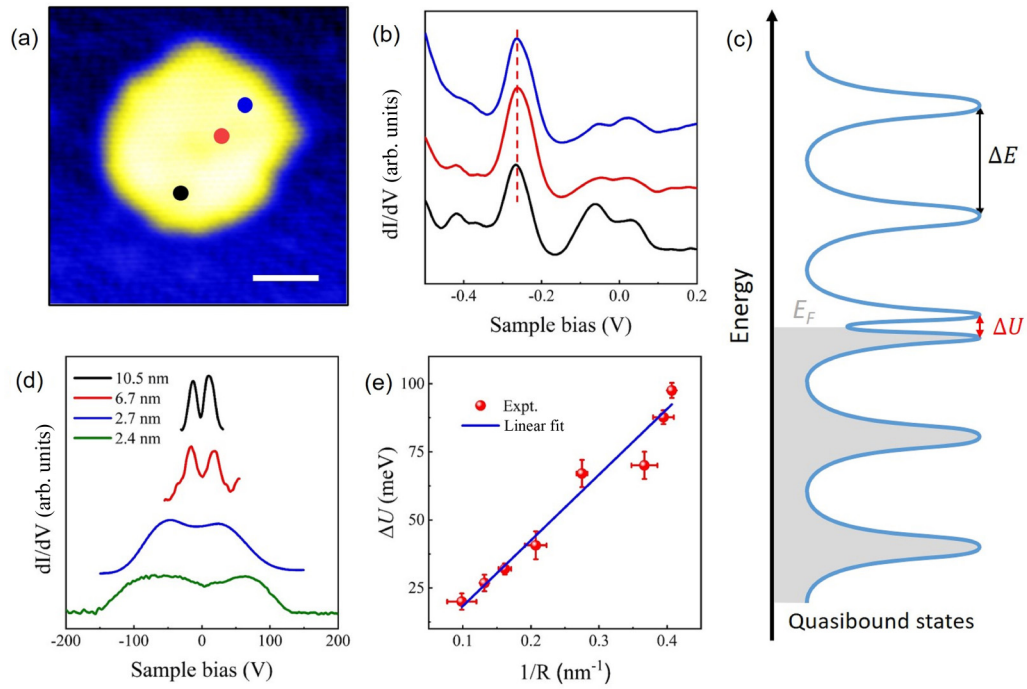

FIG. 3. Splitting of the quasibound states induced by Coulomb interaction. A STM topographic image (a) and its corresponding dI/dV spectra (b) of a GQD. (c) Illustration of filling-related splitting of the quasibound states. (d) Four normalized dI/dV spectra for the GQDs with different effective radii. For clarity, the curves are offset in the y axis. (e) Plot of average split energy as a function of the inverse effective radius for the GQDs. The data are described well by a linear fit considering Coulomb interaction in the GQDs. Scale bar: 2 nm in (a).

when it is partially filled. Figure 3(a) shows a representative STM image of a GQD and Fig. 3(b) shows the corresponding STS spectra recorded in the GQD (see Fig. S7 for the spectra in a wider range of bias voltage [31]). The energy spacing between the quasibound states, $\Delta E \sim 250$ meV, agrees well with that estimated according to $\Delta E = \hbar v_F/R$ with considering the effective radius of the GQD $R \sim 2.5$ nm, as observed in other GQDs in our experiment [Fig. 2(d)]. However, there is an obvious difference: the first quasibound state, which is partially filled, splits into two peaks with an energy separation of about 100 meV, leaving the other fully occupied quasibound states showing no signal of splitting. We can exclude the varied electric potential as the origin of the observed phenomenon because the energy of the quasibound states is almost independent of the measured positions in this GQD, as shown by the red dashed line in Fig. 3(b). We also can exclude coupling of the GQDs as the origin of the splitting because the studied GQD is quite isolated (see Fig. S8 for a larger STM image around the GQD [31]). More importantly, the coupling of the GQDs will lead to the splitting of all the quasibound states [37], which obviously differs from that observed in our work. The irregularity of the GQDs also can be excluded as the origin of the observed phenomenon because the observed splitting seems independent of the shape of the GQDs.

In our experiment, we find that the fully occupied and the completely empty quasibound states of the GQDs can be simply described by the WGM confinement and the splitting is only observed in the partially filled quasibound states, as illustrated in Fig. 3(c). The filling-related splitting in the GQDs is further confirmed in a larger GQD where the electric potential is slightly varied in the GQD, as shown in Fig. S9 [31]. One of the quasibound states changes from completely empty to fully occupied, as measured in different positions. A notable feature is that the quasibound state splits into two peaks at partial filling and does not exhibit any signal of splitting when it is empty or fully occupied. Therefore, we attribute the splitting of the partially filled quasibound states in the GQDs to the Coulomb interaction. In our experiment, the splitting of the partially filled quasibound states is observed in different GQDs with different radii, as shown in Fig. 3(d). Obviously, the splitting increases with decreasing the radius of the GQDs: the splitting increases from about 30 meV in an 8-nm GQD to about 110 meV in a 2.5-nm GQD. Previous study predicted that the Coulomb energy scales with the dot size R as $1/R$ in semiconductor quantum dots [38]. We summarized the observed splitting as a function of the radius of the GQDs in Fig. 3(e). It is interesting to note that the splitting increases linearly with the inverse effective radius of the GQDs, which can be described quite well by considering the on-site Coulomb repulsion $U = \frac{1}{4\pi\varepsilon}\frac{e^2}{R}$. Here, e is the electron charge and ε is the effective dielectric constant of the GQDs. According to the linear fitting, the effective dielectric constant of the GQDs is estimated as $\varepsilon \approx (6.62 \pm 0.25)\varepsilon_0$; here ε_0 is the vacuum dielectric constant. In previous studies [39–43], the effective dielectric constant of graphene was measured as $3\varepsilon_0 - 15\varepsilon_0$, depending on the supporting substrate (it is small in an insulating substrate and large in a conducting substrate). For simplicity, the effective dielectric constant of graphene can be estimated by $\frac{\varepsilon_0+\varepsilon_s}{2}$, where ε_s is the effective dielectric constant of the substrate [44]. For single-layer sulfur [45], the effective dielectric constant is about $2\varepsilon_0$. In our experiment, the measured effective dielectric constant

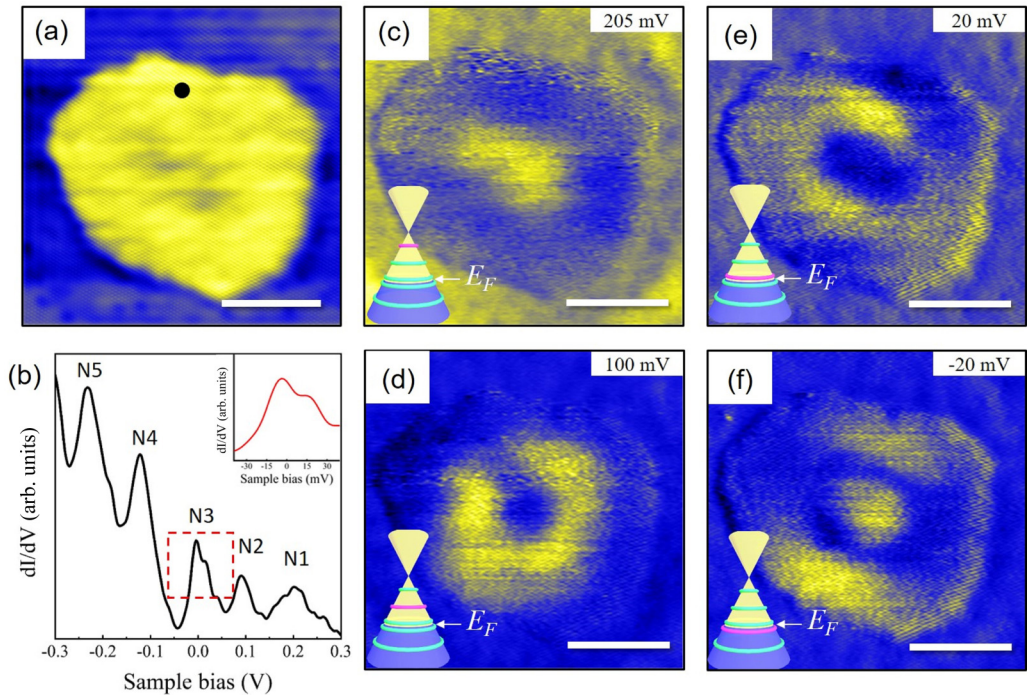

FIG. 4. Spatial distribution of LDOS recorded at the energy of empty and partially filled quasibound states. (a) A STM image of a typical GQD. (b) A dI/dV curve measured in the black point of (a) shows a series of quasibound states marked by N1–N5. The inset shows the enlarged image of N3. (c), (d) dI/dV mappings recorded at the energies of the empty quasibound states, as shown schematically in the inset. (e), (f) dI/dV mappings recorded at the energy of the two split peaks of the partially filled quasibound state. Obviously, the WGM of the quasibound state is broken. Scale bars: 5 nm.

of the GQDs is larger than the estimated value because of the copper foil beneath the S islands, which enlarges the effective dielectric constant of the S islands. According to the result in Fig. 3(e), the splitting generated by the Coulomb interaction will become quite small in large GQDs. For example, in a GQD with $R \sim 100$ nm, the splitting is only about 2 meV, which is almost undetectable in the measured spectra when considering the full width of the quasibound states. Therefore, such an effect is not observed in a large GQD [21].

Since the Coulomb interaction splits the partially filled quasibound states, it is expected that the Coulomb interaction also breaks the corresponding WGM of the quasibound states. Such an effect can be demonstrated explicitly by carrying out STS maps. Figure 4 shows representative STS maps of a GQD with the Fermi level crossing a quasibound state. As shown in Fig. 4(b), the first and the second quasibound states are fully filled, whereas the third quasibound state is half filled and a splitting on the order of 30 meV is observed. For the fully occupied and completely empty quasibound states, their STS maps exhibit the expected features as those confined via the WGM in circular GQDs, as shown in Figs. 4(c) and 4(d), respectively. However, the STS maps measured at the energies of the two split peaks of the third quasibound state show quite different features [as shown in Figs. 4(e) and 4(f)]. The shell structure, as expected for the WGM confinement of the massless Dirac fermions, is clearly broken. The states for the left peak (occupied state) and the states for the right peak (empty state) distribute separately in different regions of the GQD, which can effectively reduce the Coulomb interaction. Similar results have also been observed in other GQDs with partially filled quasibound states (see Fig. S10 for more experimental results [31]). Therefore, our experiment demonstrates that the Coulomb interaction not only splits the partially filled quasibound state, but also breaks the WGM of the corresponding quasibound state in the GQD. According to previous studies, the Coulomb interaction can lift either the spin or valley degeneracy of the quasibound states [1]. Further experiments should be carried out to explore whether the spin or valley degeneracy of the quasibound state is lifted when it is partially filled.

IV. CONCLUSIONS

In conclusion, we demonstrate that the Coulomb interaction is very important in the quasibound states of the GQDs, even though the lifetime (trapping time) of the quasibound states is only of the order of 10 fs. To reduce the Coulomb interaction, the partially filled quasibound state is split into two peaks and, simultaneously, the WGM confinement of the quasibound states is broken. In the near future, further works should be carried out to explore possible exotic phases in the GQDs induced by the Coulomb interaction.

ACKNOWLEDGMENTS

This work was supported by the National Natural Science Foundation of China (Grants No. 11974050, No. 11674029, and No. 11904075), Natural Science Foundation of Hebei Province, China (Grant No. A2019205268), and the

National Postdoctoral Program for Innovative Talents (Grant No. BX20190104). L.H. also acknowledges support from the National Program for Support of Top-notch Young Professionals, support from "the Fundamental Research Funds for the Central Universities," and support from "Chang Jiang Scholars Program."

[1] H. González-Herrero, J. M. Gómez-Rodríguez, P. Mallet, M. Moaied, J. J. Palacios, C. Salgado, M. M. Ugeda, J.-Y. Veuillen, F. Yndurain, and I. Brihuega, Atomic-scale control of graphene magnetism by using hydrogen atoms, Science **352**, 437 (2016).

[2] Y. Zhang, S.-Y. Li, H. Huang, W.-T. Li, J.-B. Qiao, W.-X. Wang, L.-J. Yin, K.-K. Bai, W. Duan, and L. He, Scanning Tunneling Microscopy of the π Magnetism of a Single Carbon Vacancy in Graphene, Phys. Rev. Lett. **117**, 166801 (2016).

[3] Y. Cao, V. Fatemi, A. Demir, S. Fang, S. L. Tomarken, J. Y. Luo, J. D. Sanchez-Yamagishi, K. Watanabe, T. Taniguchi, E. Kaxiras, R. C. Ashoori, and P. Jarillo-Herrero, Correlated insulator behaviour at half-filling in magic-angle graphene superlattices, Nature **556**, 80 (2018).

[4] Y. Cao, V. Fatemi, S. Fang, K. Watanabe, T. Taniguchi, E. Kaxiras, and P. Jarillo-Herrero, Unconventional superconductivity in magic-angle graphene superlattices, Nature **556**, 43 (2018).

[5] Y.-W. Liu, J.-B. Qiao, C. Yan, Y. Zhang, S.-Y. Li, and L. He, Magnetism near half-filling of a Van Hove singularity in twisted graphene bilayer, Phys. Rev. B **99**, 201408 (2019).

[6] G. Chen, A. L. Sharpe, P. Gallagher, I. T. Rosen, E. J. Fox, L. Jiang, B. Lyu, H. Li, K. Watanabe, T. Taniguchi, J. Jung, Z. Shi, D. Goldhaber-Gordon, Y. Zhang, and F. Wang, Signatures of tunable superconductivity in a trilayer graphene moiré superlattice, Nature **572**, 215 (2019).

[7] A. L. Sharpe, E. J. Fox, A. W. Barnard, J. Finney, K. Watanabe, T. Taniguchi, M. A. Kastner, and D. Goldhaber-Gordon, Emergent ferromagnetism near three-quarters filling in twisted bilayer graphene, Science **365**, 605 (2019).

[8] A. F. Young, C. R. Dean, L. Wang, H. Ren, P. Cadden-Zimansky, K. Watanabe, T. Taniguchi, J. Hone, K. L. Shepard, and P. Kim, Spin and valley quantum Hall ferromagnetism in graphene, Nat. Phys. **8**, 550 (2012).

[9] S.-Y. Li, Y. Zhang, L.-J. Yin, and L. He, Scanning tunneling microscope study of quantum Hall isospin ferromagnetic states in the zero Landau level in a graphene monolayer, Phys. Rev. B **100**, 085437 (2019).

[10] G. Chen, L. Jiang, S. Wu, B. Lyu, H. Li, B. L. Chittari, K. Watanabe, T. Taniguchi, Z. Shi, J. Jung, Y. Zhang, and F. Wang, Evidence of a gate-tunable Mott insulator in a trilayer graphene moiré superlattice, Nat. Phys. **15**, 237 (2019).

[11] L.-J. Yin, L.-J. Shi, S.-Y. Li, Y. Zhang, Z.-H. Guo, and L. He, High-Magnetic-Field Tunneling Spectra of ABC-Stacked Trilayer Graphene on Graphite, Phys. Rev. Lett. **122**, 146802 (2019).

[12] M. Rontani and E. Molinari, Imaging quasiparticle wave functions in quantum dots via tunneling spectroscopy, Phys. Rev. B **71**, 233106 (2005).

[13] G. Bester, D. Reuter, L. He, A. Zunger, P. Kailuweit, A. D. Wieck, U. Zeitler, J. C. Maan, O. Wibbelhoff, and A. Lorke, Experimental imaging and atomistic modeling of electron and hole quasiparticle wave functions in InAs/GaAs quantum dots, Phys. Rev. B **76**, 075338 (2007).

[14] A. Ghosal, A. D. Güçlü, C. J. Umrigar, D. Ullmo, and H. U. Baranger, Correlation-induced inhomogeneity in circular quantum dots, Nat. Phys. **2**, 336 (2006).

[15] F. Cavaliere, U. De Giovanni, M. Sassetti, and B. Kramer, Transport properties of quantum dots in the Wigner molecule regime, New J. Phys. **11**, 123004 (2009).

[16] B. Wunsch, T. Stauber, and F. Guinea, Electron-electron interactions and charging effects in graphene quantum dots, Phys. Rev. B **77**, 035316 (2008).

[17] A. D. Güçlü, P. Potasz, O. Voznyy, M. Korkusinski, and P. Hawrylak, Magnetism and Correlations in Fractionally Filled Degenerate Shells of Graphene Quantum Dots, Phys. Rev. Lett. **103**, 246805 (2009).

[18] P. Potasz, A. D. Güçlü, and P. Hawrylak, Spin and electronic correlations in gated graphene quantum rings, Phys. Rev. B **82**, 075425 (2010).

[19] T. Paananen, R. Egger, and H. Siedentop, Signatures of Wigner molecule formation in interacting Dirac fermion quantum dots, Phys. Rev. B **83**, 085409 (2011).

[20] K. A. Guerrero-Becerra and M. Rontani, Wigner localization in a graphene quantum dot with a mass gap, Phys. Rev. B **90**, 125446 (2014).

[21] Y. Zhao, J. Wyrick, F. D. Natterer, J. F. Rodriguez-Nieva, C. Lewandowski, K. Watanabe, T. Taniguchi, L. S. Levitov, N. B. Zhitenev, and J. A. Stroscio, Creating and probing electron whispering-gallery modes in graphene, Science **348**, 672 (2015).

[22] C. Gutiérrez, L. Brown, C.-J. Kim, J. Park, and A. N. Pasupathy, Klein tunnelling and electron trapping in nanometre-scale graphene quantum dots, Nat. Phys. **12**, 1069 (2016).

[23] J. Lee, D. Wong, J. Velasco, Jr., J. F. Rodriguez-Nieva, S. Kahn, H.-Z. Tsai, T. Taniguchi, K. Watanabe, A. Zettl, F. Wang, L. S. Levitov, and M. F. Crommie, Imaging electrostatically confined Dirac fermions in graphene quantum dots, Nat. Phys. **12**, 1032 (2016).

[24] K.-K. Bai, J.-J. Zhou, Y.-C. Wei, J.-B. Qiao, Y.-W. Liu, H.-W. Liu, H. Jiang, and L. He, Generating atomically sharp *p-n* junctions in graphene and testing quantum electron optics on the nanoscale, Phys. Rev. B **97**, 045413 (2018).

[25] F. Ghahari, D. Walkup, C. Gutiérrez, J. F. Rodriguez-Nieva, Y. Zhao, J. Wyrick, F. D. Natterer, W. G. Cullen, K. Watanabe, T. Taniguchi, L. S. Levitov, N. B. Zhitenev, and J. A. Stroscio, An on/off Berry phase switch in circular graphene resonators, Science **356**, 845 (2017).

[26] C. Gutiérrez, D. Walkup, F. Ghahari, C. Lewandowski, J. F. Rodriguez-Nieva, K. Watanabe, T. Taniguchi, L. S. Levitov, N. B. Zhitenev, and J. A. Stroscio, Interaction-driven quantum Hall wedding cake–like structures in graphene quantum dots, Science **361**, 789 (2018).

[27] K.-K. Bai, J.-B. Qiao, H. Jiang, H. Liu, and L. He, Massless Dirac fermions trapping in a quasi-one-dimensional *npn*

junction of a continuous graphene monolayer, Phys. Rev. B **95**, 201406 (2017).

[28] Z.-Q. Fu, Y. Zhang, J.-B. Qiao, D.-L. Ma, H. Liu, Z.-H. Guo, Y.-C. Wei, J.-Y. Hu, Q. Xiao, X.-R. Mao, and L. He, Spatial confinement, magnetic localization, and their interactions on massless Dirac fermions, Phys. Rev. B **98**, 241401 (2018).

[29] J.-J. Zhou, S. Cheng, W. You, and H. Jiang, Numerical study of Klein quantum dots in graphene systems, Sci. China Phys. Mech. Astron. **62**, 67811 (2019).

[30] D. Ma, Z. Fu, X. Sui, K. Bai, J. Qiao, C. Yan, Y. Zhang, J. Hu, Q. Xiao, X. Mao, W. Duan, and L. He, Modulating the electronic properties of graphene by self-organized sulfur identical nanoclusters and atomic superlattices confined at an interface, ACS Nano **12**, 10984 (2018).

[31] See Supplemental Material at http://link.aps.org/supplemental/10.1103/PhysRevB.101.235310 for more experimental data, analysis, theoretical calculations, and discussion.

[32] H. Walen, D.-J. Liu, J. Oh, H. J. Yang, P. M. Spurgeon, Y. Kim, and P. A. Thiel, Sulfur atoms adsorbed on Cu(100) at low coverage: characterization and stability against complexation, J. Phys. Chem. B **122**, 963 (2018).

[33] H. Walen, D.-J. Liu, J. Oh, H. Lim, J. W. Evans, Y. Kim, and P. A. Thiel, Reconstruction of steps on the Cu(111) surface induced by sulfur, J. Chem. Phys. **142**, 194711 (2015).

[34] A. F. Carley, P. R. Davies, R. V. Jones, K. R. Harikumar, G. U. Kulkarni, and M. W. Roberts, The structure of sulfur adlayers at Cu(110) surfaces: an STM and XPS study, Surf. Sci. **447**, 39 (2000).

[35] A. D. Güçlü, P. Potasz, and P. Hawrylak, Excitonic absorption in gate-controlled graphene quantum dots, Phys. Rev. B **82**, 155445 (2010).

[36] Y. Li, H. Shu, S. Wang, and J. Wang, Electronic and optical properties of graphene quantum dots: the role of many-body effects, J. Phys. Chem. C **119**, 4983 (2015).

[37] Z.-Q. Fu, Y.-T. Pan, J.-J. Zhou, D.-L. Ma, Y. Zhang, J.-B. Qiao, H. Liu, H. Jiang, and L. He, Relativistic artificial molecules realized by two coupled graphene quantum dots, arXiv:1908.06580v1.

[38] A. Francheschetti and A. Zunger, Direct Pseudopotential Calculation of Exciton Coulomb and Exchange Energies in Semiconductor Quantum Dots, Phys. Rev. Lett. **78**, 915 (1997).

[39] D. A. Siegel, C.-H. Park, C. Hwang, J. Deslippe, A. V. Fedorov, S. G. Louie, and A. Lanzara, Many-body interactions in quasi-freestanding graphene, Proc. Natl. Acad. Sci. USA **108**, 11365 (2011).

[40] Y. Wang, V. W. Brar, A. V. Shytov, Q. Wu, W. Regan, H.-Z. Tsai, A. Zettl, L. S. Levitov, and M. F. Crommie, Mapping Dirac quasiparticles near a single Coulomb impurity on graphene, Nat. Phys. **8**, 653 (2012).

[41] A. Bostwick, F. Speck, T. Seyller, K. Horn, M. Polini, R. Asgari, A. H. MacDonald, and E. Rotenberg, Observation of plasmarons in quasi-freestanding doped graphene, Science **328**, 999 (2010).

[42] D. C. Elias, R. V. Gorbachev, A. S. Mayorov, S. V. Morozov, A. A. Zhukov, P. Blake, L. A. Ponomarenko, I. V. Grigorieva, K. S. Novoselov, F. Guinea, and A. K. Geim, Dirac cones reshaped by interaction effects in suspended graphene, Nat. Phys. **7**, 701 (2011).

[43] J. P. Reed, B. Uchoa, Y. I. Joe, Y. Gan, D. Casa, E. Fradkin, and P. Abbamonte, The effective fine-structure constant of freestanding graphene measured in graphite, Science **330**, 805 (2010).

[44] E. J. G. Santos and E. Kaxiras, Electric-field dependence of the effective dielectric constant in graphene, Nano Lett. **13**, 898 (2013).

[45] D. G. Wierse, M. M. Lohrengel, and J. W. Schultze, Electrochemical properties of sulfur adsorbed on gold electrodes, J. Electroanal. Chem. **92**, 121 (1978).